KINETIC EQUILIBRIA OF ACCRETION DISCS

P. BHASKARAN and V. KRISHAN
Indian Institute of Astrophysics, Bangalore 560 034, India

(Received 27 October 1994; accepted 26 May 1995)

Abstract. A kinetic description of the equilibrium structure of accretion disc plasma is presented. It is possible to have an equilibrium configuration for a stationary axisymmetric gravitating plasma disc with spatial gradients in density, temperature and drift speed of plasma particles.

1. Introduction

Astronomical objects like x-ray sources and active galactic nuclei are powered by accretion discs around strongly gravitating bodies. Since the matter in the disc is in the plasma state, it is necessary to take into account the combined influence of the gravitational as well as the electromagnetic forces. While discussing accretion disc models for X-ray sources, Pringle and Rees (1972) have considered the influence of magnetic fields of the neutron stars on such discs in a qualitative manner. Bisnovati-Kogan and Binnikov (1972) and Ichimaru (1977) have shown that, the presence of magnetic field increases the efficiency of radiative emission. Prasanna and Bhaskaran (1989) and Bhaskaran *et al.* (1989, 1990a,b) have studied the dynamics of plasma discs around compact objects with self consistent magnetic field using the MHD approach, and shown that, the magnetic field plays an important role in the equilibrium configurations of such discs.

2. Formalism

Here, we present a study of the plasma equilibrium in accretion discs using the kinetic theory approach. We follow the method developed by Mahajan (1989) for getting exact solutions for the spatial variations of plasma parameters in different geometries. This method has been applied to the study of plasma flows in solar coronal loops by Krishan *et al.* (1991). Unlike in MHD, here it is possible to get independent variations for plasma density and temperature without using an equation of state. The kinetic approach provides a basis for investigating the micro instabilities responsible for the heating, acceleration and radiation of plasma.

It was shown by Thorne and Price (1975) that the observed hard component of the spectrum from x-ray sources like Cyg X-1 near 100 Kev can be explained if the inner portion of an accretion disc consists of optically thin high temperature gas ($T \sim 10^9 K$). Self consistent solutions for an accretion disc around a compact object with high temperature at the inner regions were obtained by Stuart and

Astrophysics and Space Science **232:** 65–78, 1995.

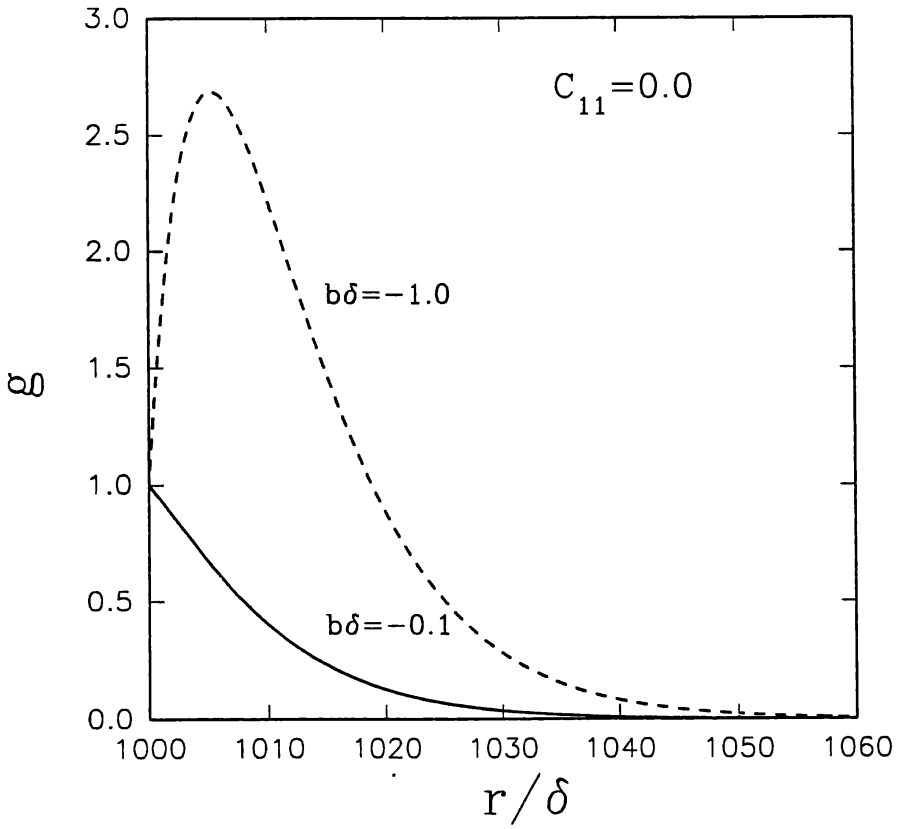

Fig. 1a. Variation of density profile function $g(r)$ versus $x = \frac{r}{\delta}$ obtained from the analytical solution for two values of $b_0\delta$.

Lightman (1976) and also they showed that in such discs the ion temperature (T_i) will be larger than the electron temperature (T_e). Here we consider a stationary axisymmetric two component plasma disc around a gravitating central object with a constant magnetic field in the z direction of the cylindrical geometry with an electron temperature $T_e \sim 10^8 K$. An inhomogeneous plasma supports different types of particle drifts and it is important to study if the plasma can remain in equilibrium in the presence of these drifts. Here, we take a nonzero drift velocity u_θ^α in the azimuthal direction in the cylindrical geometry, giving rise to the current density J_θ, which generates a magnetic field B_z. The number density n_α, the temperature T_α and the drift speed u_θ^α are spatially varying quantities, the variation in the present case being restricted to only in the radial direction. The suffix α stands for electrons and ions.

The relevant equations describing the equilibrium of a collisionless gravitating plasma permitting only radial variations $\left(\frac{\partial}{\partial\theta} = \frac{\partial}{\partial z} = 0,\ \frac{\partial}{\partial r} \neq 0\right)$ are:

$$V_r \frac{\partial f_e}{\partial r} + \vec{a}_e \cdot \frac{\partial f_e}{\partial \vec{V}} = 0 \tag{1}$$

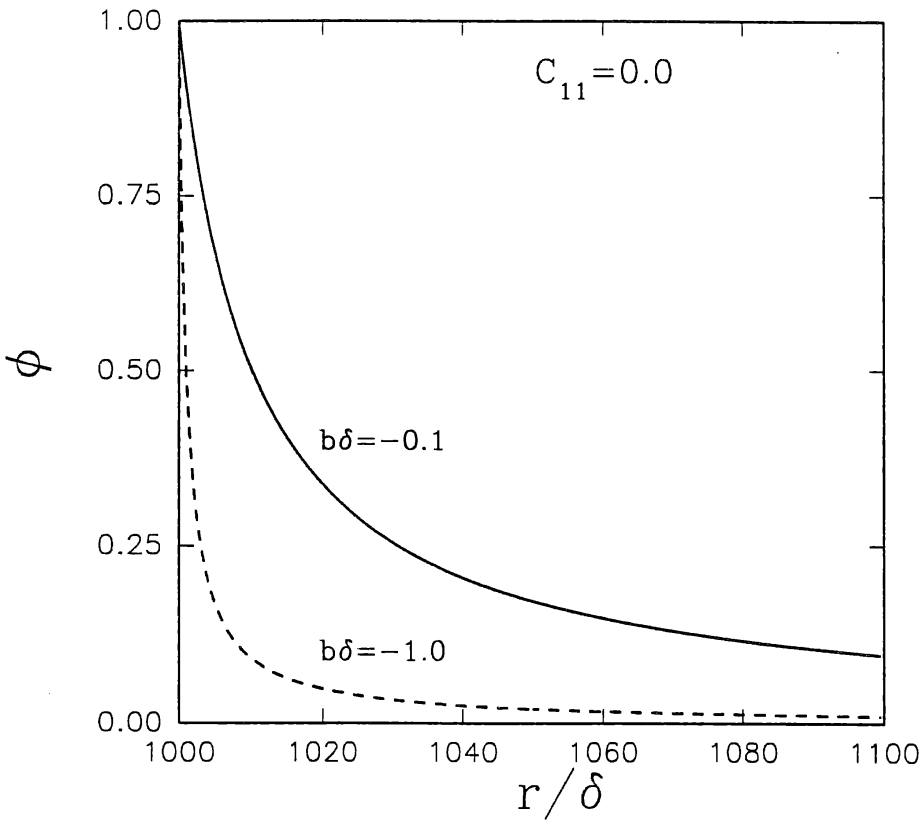

Fig. 1b. Variation of drift speed profile function $\Phi(r)$ versus $x = \frac{r}{\delta}$ obtained from the analytical solution for two values of $b_0\delta$.

$$V_r \frac{\partial f_i}{\partial r} + \vec{a}_i \cdot \frac{\partial f_i}{\partial \vec{V}} = 0 \tag{2}$$

$$\frac{dB_z}{dr} = -\frac{4\pi}{c} J_\theta \tag{3}$$

$$J_\theta = -e \int d^3 \vec{V} \, V_\theta (f_e - f_i). \tag{4}$$

where $f_{e,i}(r)$ are the single particle distribution functions for electrons and ions, $\vec{a}_{e,i}$ are their acceleration under the action of electromagnetic and any other external forces that may be present. Equations (1) and (2) are the collisionless Boltzman equations for electrons and ions respectively, Equation (3) is the Maxwell's equation and Equation (4) defines the current density in terms of the distribution functions of electrons and ions. Mahajan (1989) has shown that, for a plasma with radial gradients in temperature, density and drift speed, a series representation of the distribution function with the ratio of drift speed to thermal speed as the expansion parameter provides a solution to the Vlasov–Maxwell system of equations. When the drift speed is small compared to the thermal speed, it is possible to terminate

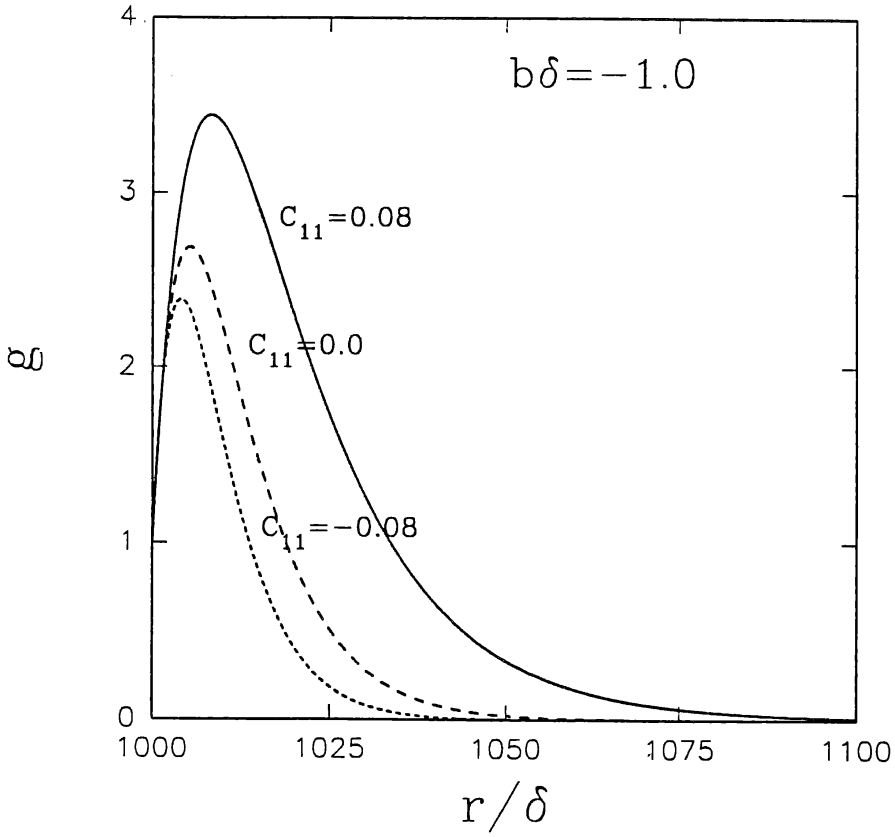

Fig. 2a. Variation of density profile function $g(r)$ versus $x = \frac{r}{\delta}$ for different values of C_{11} with $b_0\delta = -0.1$.

the series by retaining only the first few terms. We write the distribution function as:

$$f_\alpha = \frac{n_0 g}{\pi^{\frac{3}{2}}(v_{\alpha 0}^3 \Psi_\alpha^3)} \left[1 + \frac{2u_{\theta 0}^\alpha \Phi_\alpha}{v_{\alpha 0}\Psi_\alpha} \sum_{n=1}^{\infty}\sum_{m=0}^{\infty} C_{nm}^\alpha \left(\frac{V_\theta}{v_{\alpha 0}\Psi_\alpha}\right)^n \left(\frac{V}{v_{\alpha 0}\Psi_\alpha}\right)^{2m}\right] \exp\left(\frac{-V^2}{v_{\alpha 0}^2 \Psi_\alpha^2}\right. \tag{5}$$

where $g(r)$, $\Psi_\alpha(r)$ and $\Phi_\alpha(r)$ represent the spatial variations of density, thermal speed and drift speed respectively, with n_0, $v_{\alpha 0}$ and $u_{\theta 0}^\alpha$ the values of these parameters at some reference point say, r_0 the inner radius of the disc, such that,

$$g(r_0) = 1,$$

$$\Psi_\alpha(r_0) = 1,$$

$$\Phi_\alpha(r_0) = 1.$$

When both electromagnetic and gravitational forces are present, the acceleration $\vec{a}_\alpha$ is given by:

$$\vec{a}_\alpha = \frac{q_\alpha}{m_\alpha}\left(\vec{E} + \frac{\vec{V}\times\vec{B}}{c}\right) - \frac{GM}{r^2}\hat{e}_r \tag{6}$$

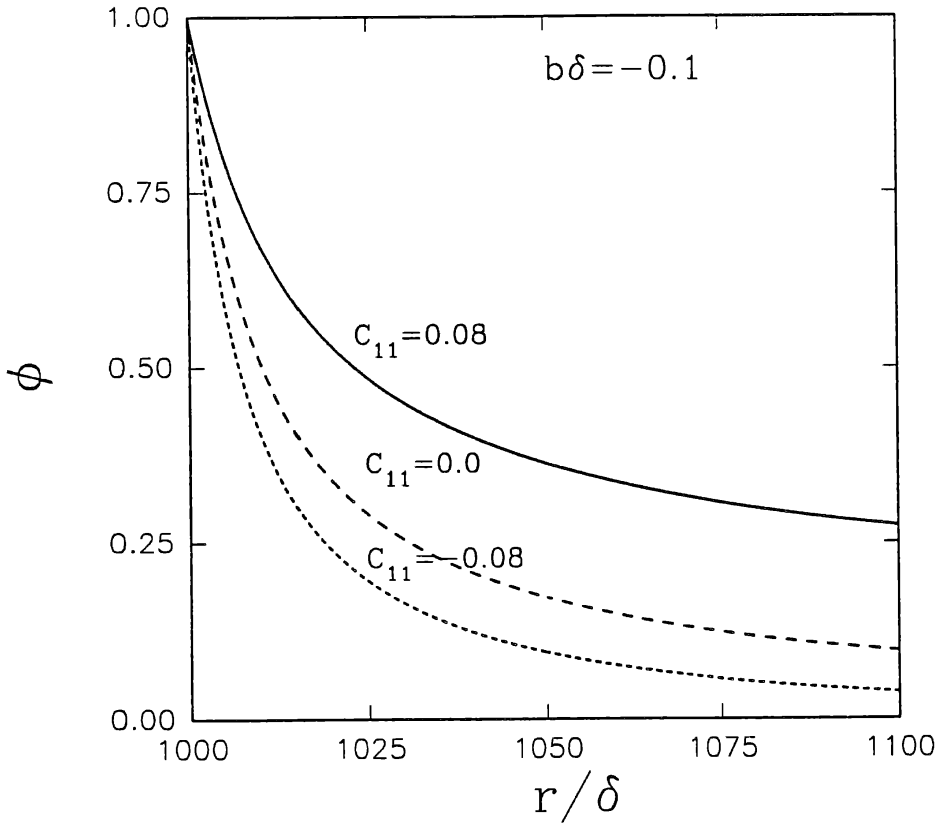

Fig. 2b. Variation of drift speed function $\Phi(r)$ versus $x = \frac{r}{\delta}$ for different values of C_{11} with $b_0\delta = -0.1$.

where M is the mass of the gravitating object, G the gravitational constant, $\vec{E}$ the electric field and $\vec{B}=\vec{B}_i + B_{z0}\hat{e}_z$ is the magnetic field consisting of the internal field B_i generated by the currents produced by the plasma motion and the externally imposed field $B_{z0}\hat{e}_z$.

Substituting Equations (5) and (6) in Equations (1) to (4) and equating the coefficients of different powers of $(u^\alpha_{\theta 0})$ to zero and retaining only terms up to first order in $\left(\frac{u^\alpha_{\theta 0}\Phi_\alpha}{v_{\alpha 0}\Psi_\alpha}\right)$ gives the following set of differential equations:

$$\frac{\Psi_\alpha^3}{g}\frac{d}{dr}\left(\frac{g}{\Psi_\alpha^3}\right) + \frac{2}{v_{\alpha 0}^2\Psi_\alpha^2}\left(\frac{GM}{r^2} - \frac{q_\alpha E_r}{m_\alpha}\right) = C_{10}^\alpha \frac{2q_\alpha u^\alpha_{\theta 0} B_z \Phi_\alpha}{c m_\alpha v_{\alpha 0}^2 \Psi_\alpha^2} \tag{7}$$

$$\frac{2}{\Psi_\alpha}\frac{d\Psi_\alpha}{dr} = C_{11}^\alpha \frac{2q_\alpha u^\alpha_{\theta 0} B_z \Phi_\alpha}{c m_\alpha v_{\alpha 0}^2 \Psi_\alpha^2} \tag{8}$$

$$\frac{1}{\Phi_\alpha}\frac{d\Phi_\alpha}{dr} - \frac{1}{r} - \frac{C^\alpha}{C_{10}^\alpha}\frac{2}{v_{\alpha 0}^2\Psi_\alpha^2}\left(\frac{GM}{r^2} - \frac{q_\alpha E_r}{m_\alpha}\right) - \frac{C_{20}^\alpha}{C_{10}^\alpha}\frac{2q_\alpha B_z}{c m_\alpha v_{\alpha 0}\Psi_\alpha} =$$

$$(C_{11}^\alpha - C_{10}^\alpha)\frac{2q_\alpha u^\alpha_{\theta 0} B_z \Phi_\alpha}{c m_\alpha v_{\alpha 0}^2 \Psi_\alpha^2} \tag{9}$$

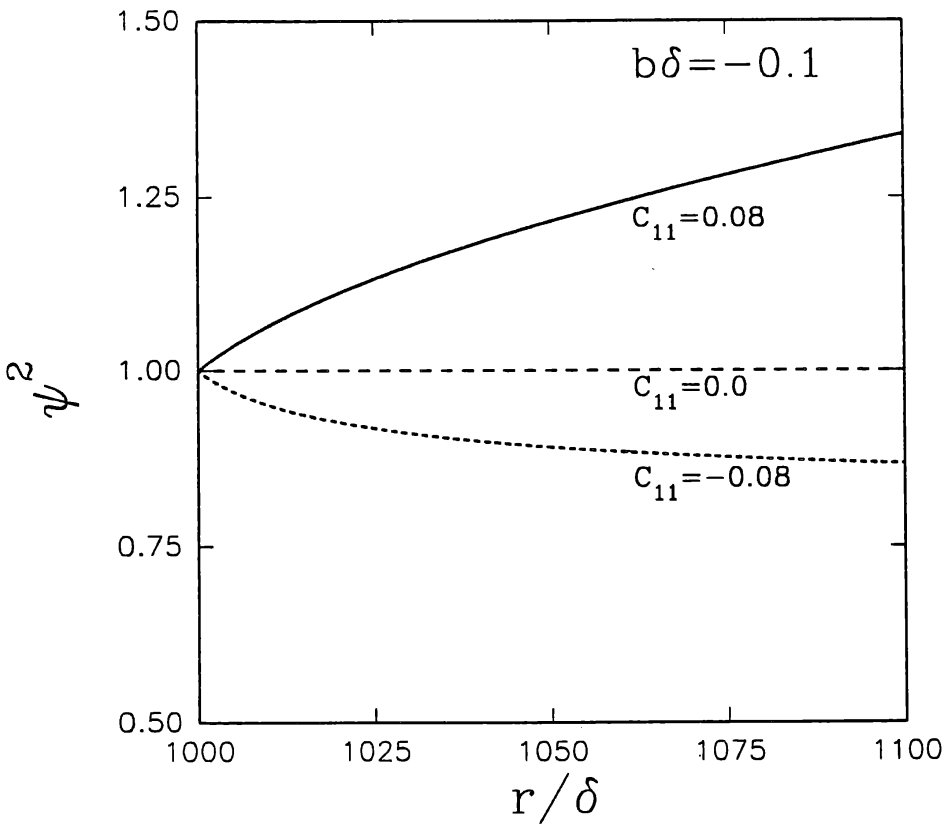

Fig. 2c. Variation of Temperature profile function $\Psi^2(r)$ versus $x = \frac{r}{\delta}$ for different values of C_{11} with $b_0\delta = -0.1$.

$$\frac{dB_z}{dr} = \frac{4\pi}{c} e n_0 g \left[u^e_{\theta 0} \Phi_e \left(C^e_{10} + \frac{5}{2} C^e_{11} \right) - u^i_{\theta 0} \Phi_i \left(C^i_{10} + \frac{5}{2} C^i_{11} \right) \right] \tag{10}$$

$$C^\alpha_{21} = C^\alpha_{11} \frac{u^\alpha_{\theta 0} \Phi_\alpha}{v_{\alpha 0} \Psi_\alpha} \left[2C^\alpha_{10} - 2C^\alpha_{11} + \frac{C^\alpha_{11}}{2} \left(\frac{1}{\Psi_\alpha} \frac{d\Psi_\alpha}{dr} \right)^{-1} \left(\frac{1}{\Phi_\alpha} \frac{d\Phi_\alpha}{dr} - \frac{1}{r} \right) \right] \tag{11}$$

$$C^\alpha_{22} = (C^\alpha_{11})^2 \frac{u^\alpha_{\theta 0} \Phi_\alpha}{v_{\alpha 0} \Psi_\alpha}. \tag{12}$$

All C^α_{nm}, for which $m \geq n + 1$ turn out to be zero.

The number density, drift speed and temperature are defined in terms of the distribution function as follows.

$$n_\alpha = \int f_\alpha d\vec{V} \tag{13}$$

$$n_\alpha \bar{V}_\alpha = \int f_\alpha \vec{V}_\alpha \, d\vec{V} \tag{14}$$

$$\frac{3}{2} n_\alpha K T_\alpha = \int \frac{1}{2} m_\alpha V^2 f_\alpha d\vec{V} \tag{15}$$

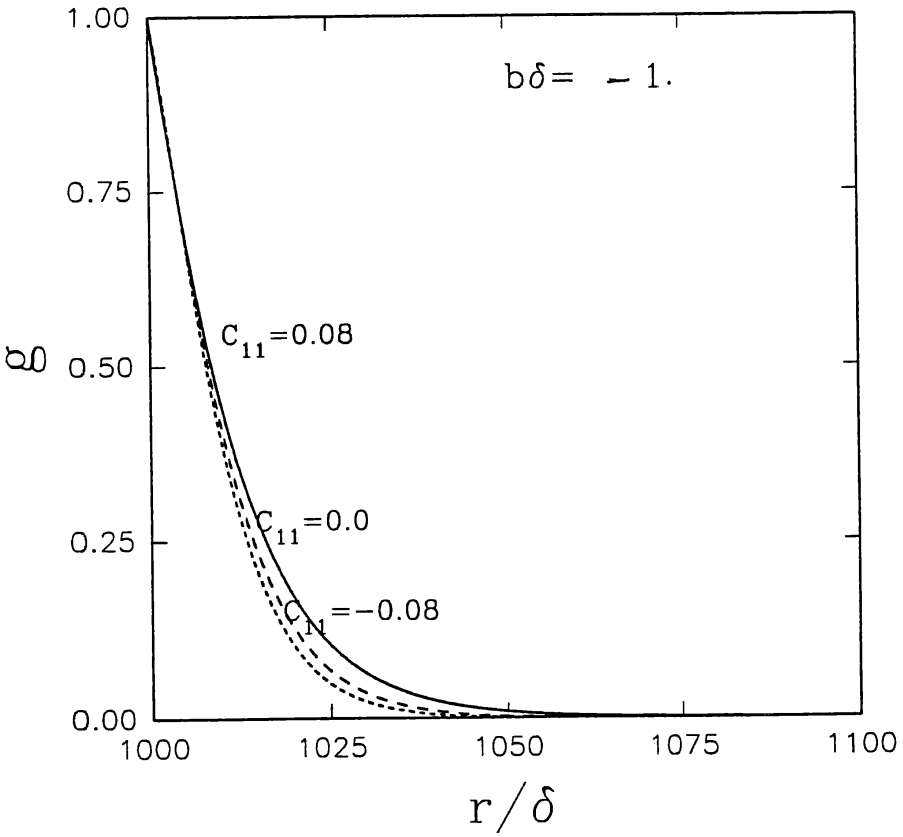

Fig. 3a. Variation of density profile function $g(r)$ versus $x = \frac{r}{\delta}$ for different values of C_{11} with $b_0\delta = -1.0$.

For the distribution function given by equation (5) we get, up to first order in $\left(\frac{u^\alpha_{\theta 0}\Phi_\alpha}{v_{\alpha 0}\Psi_\alpha}\right)$,

$$n_\alpha = n_0 g \tag{16}$$

$$n_\alpha \bar{V}_\alpha = n_0 g u^\alpha_{\theta 0}\Phi_\alpha \left(C^\alpha_{10} + \frac{5}{2}C^\alpha_{11}\right) \tag{17}$$

$$\frac{KT_\alpha}{m_\alpha} = \frac{1}{2}v^2_{\alpha 0}\Psi^2_\alpha \tag{18}$$

We choose $C^\alpha_{10} + \frac{5}{2}C^\alpha_{11} = 1$, so that $u^\alpha_{\theta 0}\Phi_\alpha$ represents the drift speed. Also we assume $C^\alpha_{20} = 0$. Since we are interested in the equilibrium solutions we will assume that at equilibrium $\Phi_e = \Phi_i$ and $\Psi_e = \Psi_i$, i.e., electrons and ions have the same spatial profiles. Also, it is assumed that the expansion coefficients C^α_{1m} are same for electrons and ions. From Equations (7) and (8) we find the conditions:

$$\frac{u^i_{\theta 0}}{u^e_{\theta 0}} = -\frac{T_{i0}}{T_{e0}} = -\tau_0 \tag{19}$$

$$\frac{2eE_r}{m_e v^2_{e0}\Psi^2} = -\left(\frac{\tau_0 - \frac{m_i}{m_e}}{\tau_0 + 1}\right)\frac{2GM}{m_e v^2_{e0}\Psi^2 r^2} \tag{20}$$

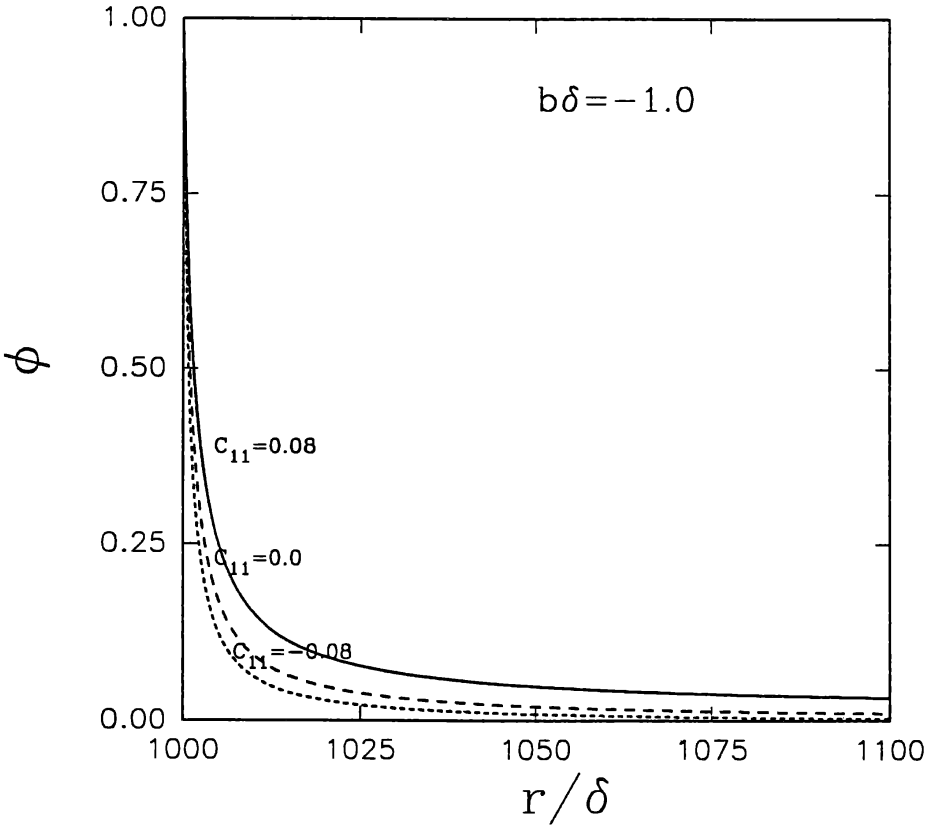

Fig. 3b. Variation of drift speed profile function $\Phi(r)$ versus $x = \frac{r}{\delta}$ for different values of C_{11} with $b_0\delta = -1.0$.

Equation (20) shows that the charge neutrality condition introduces an electric field in the disc whose strength depends on the parameter $\tau_0 = \frac{T_{i0}}{T_{e0}}$. The electric field is zero when $\tau_0 = \frac{m_i}{m_e}$,

Now the set of Equations (7) to (10) reduces to

$$\frac{1}{g}\frac{dg}{dr} + \frac{\left(1+\frac{m_i}{m_e}\right)}{(1+\tau_0)}\frac{2}{v_{e0}^2\psi^2}\frac{GM}{r^2} = -\left(C_{10}+\frac{3}{2}C_{11}\right)\frac{b\Phi}{\Psi^2} \tag{21}$$

$$\frac{2}{\Psi}\frac{d\Psi}{dr} = -C_{11}\frac{b\Phi}{\Psi^2} \tag{22}$$

$$\frac{1}{\Phi}\frac{d\Phi}{dr} - \frac{1}{r} - \frac{C_{11}}{C_{10}}\frac{\left(1+\frac{m_i}{m_e}\right)}{(1+\tau_0)}\frac{2}{v_{e0}^2\Psi^2}\frac{GM}{r^2} = (C_{10}-C_{11})\frac{b\Phi}{\Psi^2} \tag{23}$$

$$\frac{dB_z}{dr} = \frac{4\pi}{c}en_0u_{\theta 0}^e(1+\tau_0)g\Phi \tag{24}$$

where $b = \frac{2eB_zu_{\theta 0}^e}{cm_ev_{e0}^2}$, and plasma frequency, $\omega_{pe} = \left(\frac{4\pi n_0e^2}{m_e}\right)^{\frac{1}{2}}$. δ is an effective skin depth of plasma.

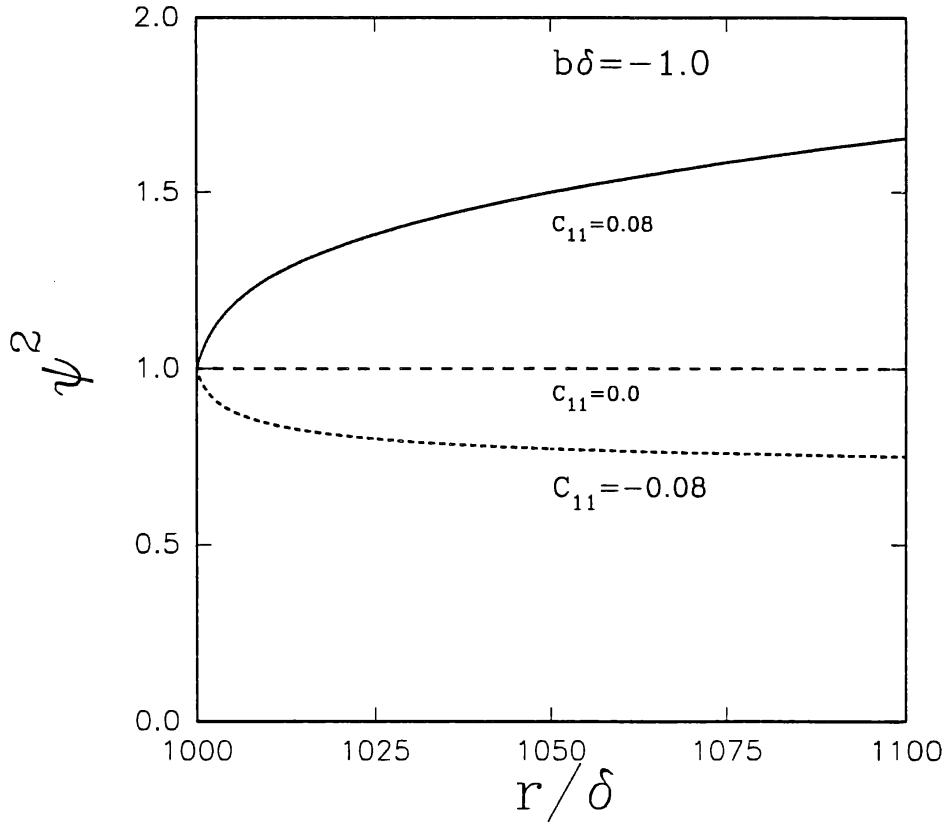

Fig. 3c. Variation of temperature profile function $\Psi^2(r)$ versus $x = \frac{r}{\delta}$ for different values of C_{11} with $b_0\delta = -1.0$.

For the present study we assume that the external field B_{z0} is much larger than the internal field produced by the currents B_{zi} and we make the approximation $b \sim b_0 = \frac{2eB_{z0}u^e_{\theta 0}}{cm_e v^2_{e0}}$. Now the set of Equation (21) to (24) in terms of the dimensionless parameter $x = \frac{r}{\delta}$ can be written as:

$$\frac{1}{g}\frac{dg}{dx} + \frac{\beta}{x^2\Psi^2} = -\left(C_{10} + \frac{3}{2}C_{11}\right)\frac{b_0\delta\Phi}{\Psi^2} \tag{25}$$

$$\frac{2}{\Psi}\frac{d\Psi}{dx} = -C_{11}\frac{b_0\delta\Phi}{\Psi^2} \tag{26}$$

$$\frac{1}{\Phi}\frac{d\Phi}{dx} - \frac{1}{x} - \frac{C_{11}}{C_{10}}\frac{\beta}{x^2\Psi^2} = (C_{10} - C_{11})\frac{b_0\delta\Phi}{\Psi^2} \tag{27}$$

$$\frac{db}{dx} = 2g\Phi \tag{28}$$

where $\delta = \frac{c\omega_{pe}}{v_{e0}u^e_{\theta 0}(1+\tau_0)^{\frac{1}{2}}}$, and $\beta = \frac{\left(1+\frac{m_i}{m_e}\right)}{(1+\tau_0)}\frac{2GM}{v^2_{e0}\delta}$.

From Equations (25) to (27) we get an expression for the spatial profile of temperature Ψ^2 in terms of g and Φ as given by:

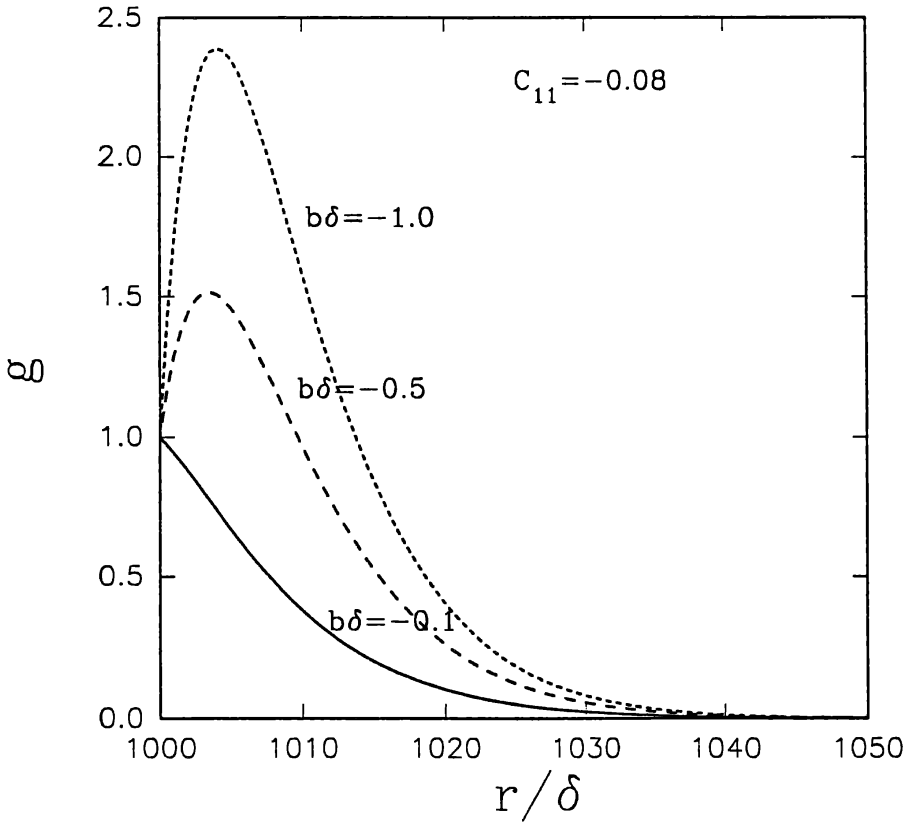

Fig. 4a. Variation of density profile function $g(r)$ versus $x = \frac{r}{\delta}$ for different values of magnetic field with $C_{11} = -0.08$.

$$\Psi^2 = \left[\left(\frac{r}{r_0}\right) \Phi g^{\frac{C_{11}}{C_{10}}}\right]^{\frac{2c_{10}C_{11}}{3C_{11}^2 - 2C_{10}^2 + 4C_{10}C_{11}}} \tag{29}$$

For $C_{11} = 0$, which corresponds to a disc with constant temperature Equations (25) and (27) can be solved to get analytical solutions for the spatial profiles for number density and drift speed as given by:

$$g = \left[1 + b_0\delta\frac{x_0}{2}\left(1 - \frac{x2}{x_0^2}\right)\right] \exp\left(\frac{\beta}{x} - \frac{\beta}{x_0}\right) \tag{30}$$

$$\Phi = \left(\frac{x}{x_0}\right)\left[1 + b_0\delta\frac{x_0}{2}\left(1 - \frac{x2}{x_0^2}\right)\right]^{-1} \tag{31}$$

For the case with $C_{11} \neq 0$ corresponding to a disc with spatial variation in temperature the Equations (25) and (27) were solved numerically and the spatial profiles of number density and drift speed were obtained. The temperature is given by the relation (29) and the pressure profile obtained from the relation: Pressure $\propto g\Psi^2$.

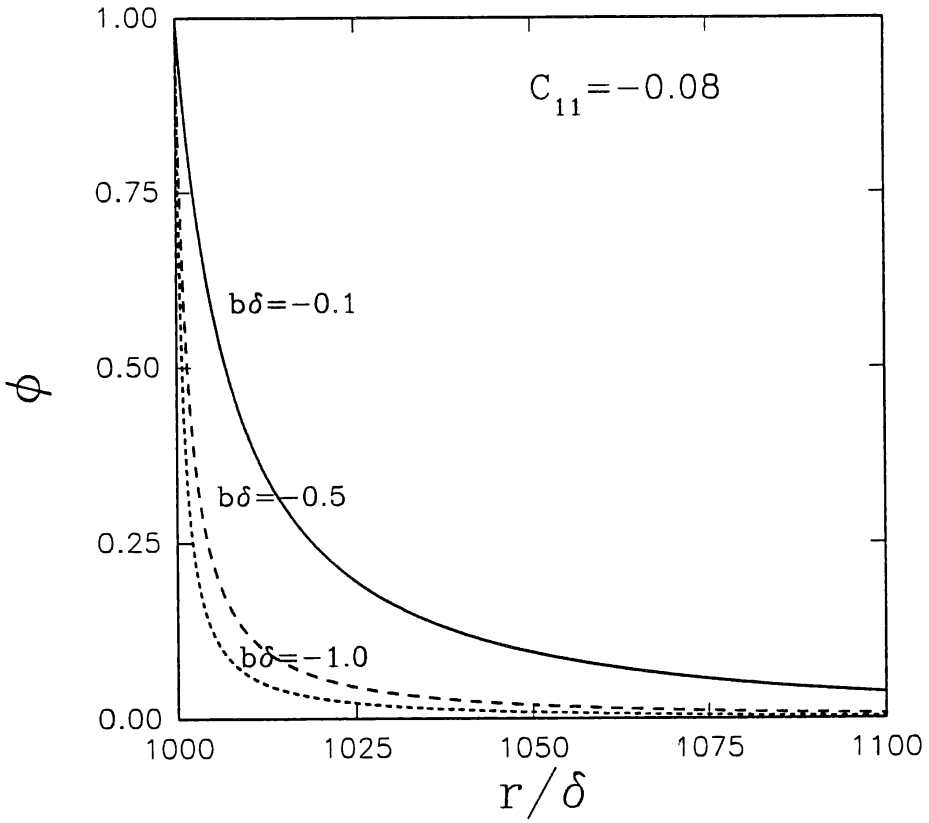

Fig. 4b. Variation of drift speed profile function $\Phi(r)$ versus $x = \frac{r}{\delta}$ for different values of magnetic field with $C_{11} = -0.08$.

3. Results and Discussions

We have considered a plasma disc around a neutron star, with the inner radius (r_0) of the disc at 10^6 cm. At the inner boundary $g = \Psi = \Phi = 1$. We assume an electron density $n_0 = 10^{10}$ particle/cm^3, an electron temperature $T_e = 10^8 K$ and ion temperature $T_i = 10^{10} K$ at the inner boundary. The corresponding electron and ion thermal speeds are $v_{e0} = 5.5 \times 10^9$ cm/s and $v_{i0} = 1.285 \times 10^9$ cm/s. The drifting Maxwellian can exist for time scales smaller than the collision time $(\nu_{ei})^{-1}$, where the collision frequency ν_{ei} is given by $\nu_{ei} = \frac{4}{\sqrt{2}} \left(\frac{\pi}{3}\right)^{\frac{3}{2}} Z^2 \frac{e^4}{m_i} \left(\frac{m_i}{KT}\right)^{\frac{3}{2}} N_i g(\nu, T) \sim 50 N_i T^{-\frac{3}{2}}$. For stability of the plasma against microscopic instabilities electron drift speed $u^e_{\theta 0}$ should be less than the ion sound speed given by $c_s = \left(\frac{k_B T_e}{m_i}\right)^{\frac{1}{2}}$, which is 9.1×10^7 cm/s in the present case. The condition that the characteristic drift time $\frac{\delta}{u^e_{\theta 0}} < (\nu_{ei})^{-1}$ and $u^e_{\theta 0} < c_s$ restricts $u^e_{\theta 0}$ to 5×10^2 cm/s $< u^e_{\theta 0} < 9.1 \times 10^7$ cm/s. With electron drift speed $u^e_{\theta 0} = 3 \times 10^6$ cm/s, we get:

$\delta = 10^3$ cm,
$t_{\text{coll}} = 2$s,
$t_{\text{drift}} = 3.42 \times 10^{-4}$s.

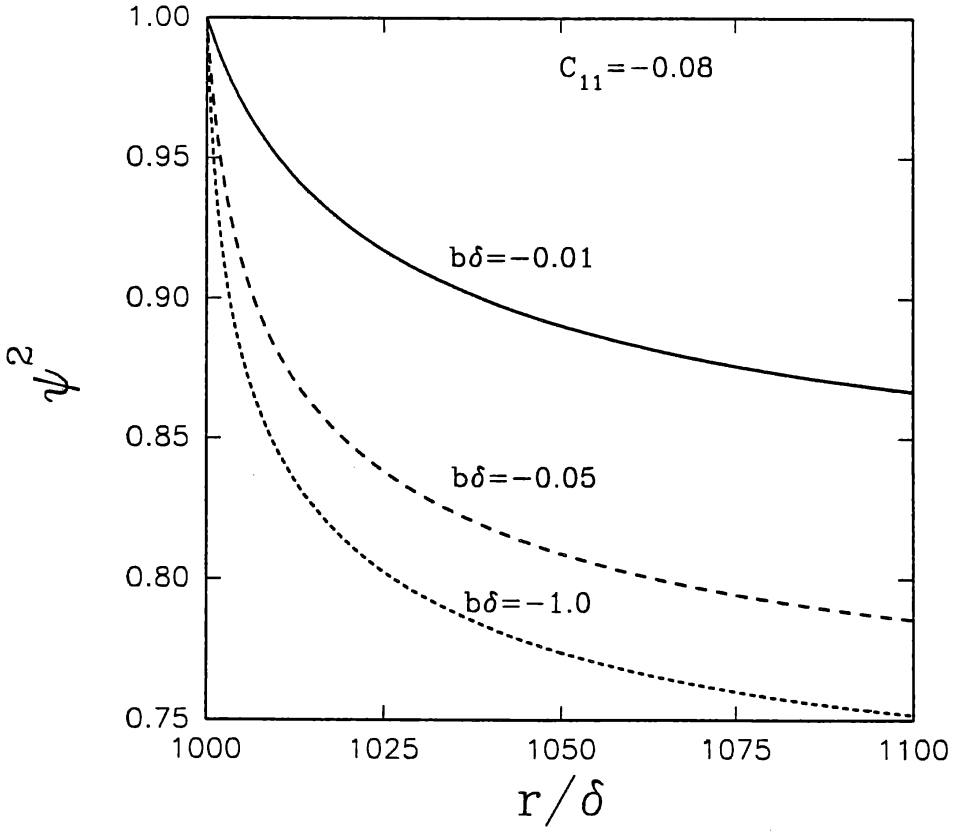

Fig. 4c. Variation of temperature profile function $\Psi^2(r)$ versus $x = \frac{r}{\delta}$ for different values of magnetic field with $C_{11} = -0.08$.

For a solar mass neutron star $\beta = 1.62 \times 10^5$. The relation between magnetic field strength B_z and the dimensionless parameter $b_0\delta$ is given by: $B_z = 500(b_0\delta)$ Gauss. The rotational velocity u_θ of the plasma around the central gravitating object can be obtained from the drift velocities of the ions and electrons using the relation $u_\theta = \frac{m_i n_i u_\theta^i + m_e n_e u_\theta^e}{m_i n_i + m_e n_e}$. For the parameters that we had chosen $u_\theta \sim u_\theta^i$ and at the inner boundary of the disc $u_\theta^i = u_{\theta 0}^i = 3 \times 10^8$ cm/s.

We note that the Debye length $\lambda_D = \frac{v_{e0}}{\omega_{pe}} = 1$ cm, which is much smaller than $\delta = 10^3$ cm. There for it is justified to neglect charge separation effects, for the equilibrium. However charge separation effects will have to be included while studying the stability of the equilibrium.

The characteristic time scales over which microscopic instabilities occur are determined by the electron plasma (ω_{pe}) and ion plasma (ω_{pi}) frequencies, both of which are much larger than the collision frequency ν_{ei}. Thus the relevant equilibrium configuration which may become unstable against microscopic instabilities, is described by the drifting Maxwellian, instead of thermal Maxwellian.

Figures 1a and 1b show the spatial profiles of number density and drift speed given by the analytical solution for the case of a constant temperature disc, for two different values of the magnetic field. The drift speed shows the same behavior,

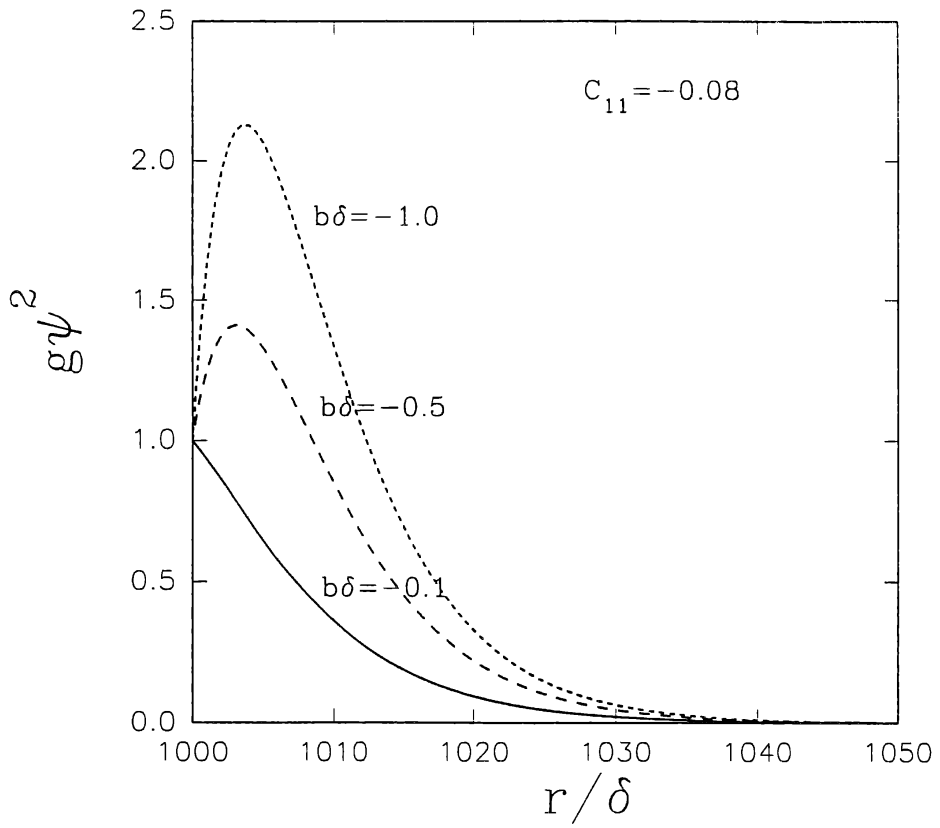

Fig. 5. Variation of pressure profile function $g(r)\Psi^2(r)$ versus $x = \frac{r}{\delta}$ for different values of magnetic field with $C_{11} = -0.08$.

i.e., decreasing with increasing $x = \frac{r}{\delta}$, in both cases. For $b_0\delta = -0.1$ which corresponds to $B_{z0} \sim -50$ Gauss, the number density decrease as x is increased. For $b_0\delta = -1.0$ corresponding to $B_{z0} \sim -500$ Gauss, the number density increases for some time and then stars decreasing.

Figures 2a to 2c show the spatial profiles of number density, drift speed and temperature for different values of C_{11} with $b_0\delta = -0.1$. $C_{11} < 0$ and $C_{11} > 0$ corresponds respectively to discs with increasing or decreasing temperature with increase in x, while $C_{11} = 0$ corresponds to constant temperature disc. Figures 3a to 3c show the same profiles for the case $b_0\delta = -1.0$.

Figures 4a to 4c show the spatial profiles of number density, drift speed, and temperature for different values of magnetic field. As magnetic field is increased the drift speed and temperature decrease faster. For large magnetic fields, the number density increase for some distance and then starts decreasing.

Figure 5 shows spatial profiles of pressure for different values of magnetic field. Figure 4a and Figure 5 show that, at the inner edge of the disc, the spatial profiles of density and pressure depend on the strength of the magnetic field present. While for small magnetic field strength, density and pressure increase continuously towards the inner edge, for large field strengths they reach a maximum value and then decrease rapidly. This shows that the disc structure gets disrupted in the presence

of strong magnetic fields, and agrees with the result obtained using the MHD approach by Bhaskaran *et al.* (1990a,b).

Here we have shown that it is possible to get equilibrium configurations of plasma discs with spatial variations in number density, temperature and drift speed using the kinetic approach. It is shown that the spatial profiles of the number density and pressure in the disc, and hence the structure of the disc depends on the strength of the magnetic field. Using kinetic approach it is possible to get the temperature and number density distribution separately without using an equation of state.

4. Conclusions

Kinetic equilibria of accretion disc plasma have been determined under the assumptions of quasineutrality and absence of collisionality. These equilibria stay for times which are much smaller than the collisional time but much larger than the time scales of the microinstabilities which can heat and accelerate the plasma particles extremely rapidly.

In this study we have neglected the effects of the self consistent magnetic field generated by the currents due to motion of the plasma, on the structure and dynamics of the disc. We are trying to extend our analysis to plasma disc systems with spatial variations of the plasma parameters in both r and z directions, and also including self consistent magnetic field with proper boundary conditions.

Acknowledgement

One of the authors (P. Bhaskaran) is grateful to CSIR, (India), for the award of a research associateship, during the tenure of which the present work has been done.

References

Bhaskaran, P. and Prasanna, A.R.: 1989, *Astrophys. Space Sci.* **159**, 109.
Bhaskaran, P. and Prasanna, A.R.: 1990a, *Astrophys. Astro.* **11**, 49.
Bhaskaran, P., Thripathy, S.C., and Prasanna, A.R.: 1990b, *J. Astrophys. Astron.* **11**, 461.
Bisnovathy Kogan, G.S. and Binnikov, S.I.: 1972, *Astrophys. Space Sci.* **19**, 119.
Ichimaru, S.: 1977, *Astrophys. J.* **214**, 840.
Krishan, V., Sreedharan, T.D., and Mahajan, S.M.: 1991, *Monthly Notices Roy. Astron. Soc.* **249**, 596.
Mahajan, S.M.: 1989, *Phys. Fluids, B1* **1**, 43.
Prasanna, A.R. and Bhaskaran, P.: 1989, *Astrophys. Space Sci.* **153**, 201.
Pringle, J.E. and Rees, M.J.: 1972, *Astron. Astrophys.* **21**, 1.
Shapiro, S.L. and Lightman, A.P.: 1976, *Ap. J.* **204**, 187.
Thorne, K.S. and Price, R.H.: 1975, *Ap. J. (Letters)* **195**, L101.